

TRAFFIC DATA AND THEIR IMPLICATIONS FOR CONSISTENT TRAFFIC FLOW MODELING

Dirk Helbing^{*,1}

** II. Institute of Theoretical Physics, University of Stuttgart,
Pfaffenwaldring 57/III, 70550 Stuttgart, Germany,
www: <http://www.uni-stuttgart.de/UNIuser/thphys/helbing.html>*

Abstract: The paper analyzes traffic data with respect to certain aspects which are relevant for traffic flow modeling as well as the calibration of model parameters and functions. Apart from the dynamic velocity distribution, the density-dependence and the temporal evolution of various, partly lane-specific quantities is investigated. The results are well compatible with recent macroscopic traffic flow models which have been derived from the dynamics of driver-vehicle units. These have also solved the inconsistencies, which previous models have been criticized for.

Keywords: Calibration, consistency, evaluation, mathematical models, vehicle dynamics

1. INTRODUCTION

Efficient traffic flow is very important for a high standard of living. However, during the last decades the traffic volume has continuously increased, so that the capacity of the road system is almost reached in many countries, especially in conurbations. Therefore, methods for traffic flow optimization are called for. To develop these, numerous traffic simulation models have been proposed.

This paper will focus on macroscopic (fluid-dynamic) models for the vehicle density and the average velocity. It addresses essentially two questions: 1. Which phenomena and functional relations should be reproduced by the models? Related results are presented in the next section. 2. Which one of the existing traffic flow models should be used to simulate traffic dynamics? This is the topic of Sect. 3. In particular, it is discussed which consistency requirements should be met by realistic models.

2. DATA EVALUATION

During the last year single vehicle data of the Dutch two-lane Autobahn A9 from Haarlem to Amsterdam have been evaluated with respect to various criteria which are relevant for traffic flow modeling. The quantities measured by induction loops at discrete places x along the freeway include the passage times $t_\alpha(x)$, velocities $v_\alpha(x)$, vehicle lengths $l_\alpha(x)$, and lanes $i_\alpha(x)$ of the single vehicles α . These allow the determination of various aggregate (so-called macroscopic) quantities.

The results of the standard evaluation methods have already been presented, compared and discussed elsewhere (Helbing, 1997). They base on averages over a fixed time interval T , giving large statistical variations of the velocity moments

$$\langle v^k \rangle = \frac{1}{N(x, t)} \sum_{t-T/2 \leq t_\alpha < t+T/2} [v_\alpha(x)]^k \quad (1)$$

where the traffic flow $Q(x, t) = N(x, t)/T$ is small, since the number $N(x, t)$ of vehicles passing the intersection at place x between times $t - T/2$ and $t + T/2$ is small, then.

¹ The author is grateful to Henk Taale and the Ministry of Transport, Public Works and Water Management for supplying the freeway data.

The following considerations will focus on an evaluation method with a sampling error that is independent of the traffic volume. For this purpose, one averages over a fixed number $N = 100$ of vehicles, implying a variation of the time interval $T(x, t)$ of data collection. Then, the definition of the space- and time-dependent traffic flow is $Q(x, t) = N/T(x, t)$ with

$$t = \frac{1}{N} \sum_{\alpha_0 \leq \alpha < \alpha_0 + N} t_\alpha(x), \quad (2)$$

and the velocity moments are given by

$$\langle v^k \rangle = \frac{1}{N} \sum_{\alpha_0 \leq \alpha < \alpha_0 + N} [v_\alpha(x)]^k. \quad (3)$$

This allows the calculation of the average velocity $V(x, t) = \langle v \rangle$, the density $\rho(x, t) = Q(x, t)/V(x, t)$, the velocity variance

$$\Theta(x, t) = \langle [v - V(x, t)]^2 \rangle = \langle v^2 \rangle - \langle v \rangle^2, \quad (4)$$

the skewness

$$\gamma(x, t) = \frac{\langle [v - V(x, t)]^3 \rangle}{[\Theta(x, t)]^{3/2}}, \quad (5)$$

and the kurtosis

$$\delta(x, t) = \frac{\langle [v - V(x, t)]^4 \rangle}{[\Theta(x, t)]^2} - 3. \quad (6)$$

The definitions for the single lanes i are analogous to the above ones for the total cross section.

Whereas the variance Θ is a measure for the breadth of the velocity distribution $P(v; x, t)$, the skewness is a measure for its asymmetry, and the kurtosis for its flatness. Most previous studies have restricted to the evaluation of the velocity-density relation $V_e(\rho)$ (Fig. 1) and the fundamental diagram $Q_e(\rho)$ (Fig. 2).

However, for some theoretical considerations, it is essential to know the form of the velocity distribution in dependence of density. In agreement with previous studies it was found that a normal distribution is a good approximation for the average velocity distribution (Fig. 3). Recent numerical solutions for the stationary velocity distribution of an improved kinetic traffic model yield similar results (Fig. 4).

Due to the limited amount of data, the *time-dependent* velocity distribution is hard to obtain. Therefore, it has been investigated whether the time-dependent skewness (Fig. 5) and the kurtosis (Fig. 6) vanish in agreement with a normal distribution. The deviation of the skewness from zero is indeed neither systematic nor significant. The kurtosis is also very small but, on average, somewhat smaller than zero. Since this systematic

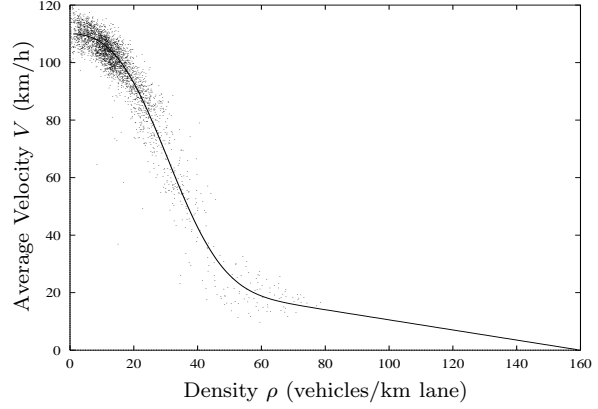


Fig. 1. Empirical velocity-density data (\cdot) for the Dutch two-lane freeway A9 with a speed limit of 120 km/h. The fit function $V_e(\rho)$ (—) at high densities is reconstructed by means of theoretical traffic flow relations (cf. Sect. 3).

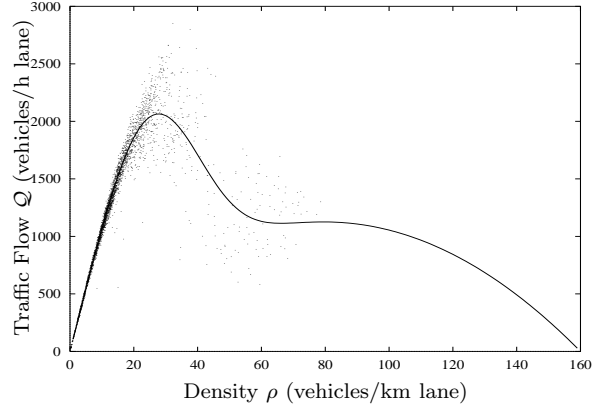


Fig. 2. Empirical flow-density data (\cdot) and fit of the fundamental diagram $Q_e(\rho)$ (—).

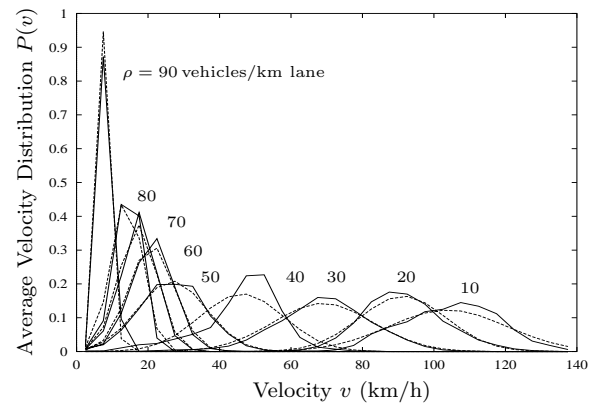


Fig. 3. Comparison of empirical velocity distributions at different densities (—) with frequency polygons of grouped normal distributions having the same mean value and variance (---). A significant deviation of the empirical relations from the respective discrete normal approximations is only found at $\rho = 40$ vehicles/km lane, where the averaging interval T may have been too long due to rapid stop-and-go waves (cf. the mysterious “knee” at $\rho \approx 40$ vehicles/km lane in Fig. 7).

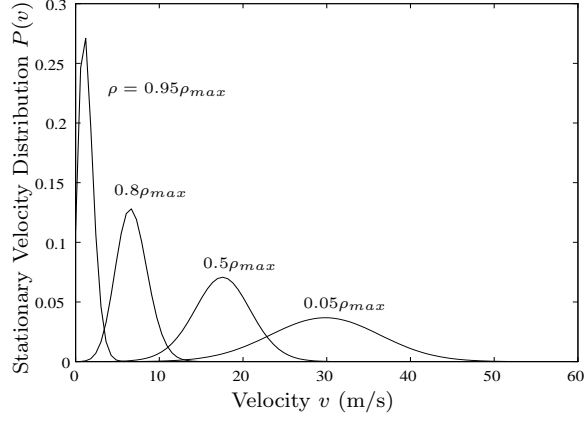


Fig. 4. Stationary velocity distributions at different vehicle densities obtained from a improved kinetic traffic model (reproduction by kind permission of C. Wagner).

deviation from zero can be shown to vanish on the left-hand lane, it is probably an effect of the finite truck fraction driving slower than other vehicles.

In summary, the velocities are almost normally distributed, even in the dynamic case. Nevertheless, if one averages over too large time intervals T , bimodal distributions may result in cases of strong variations of traffic flow.

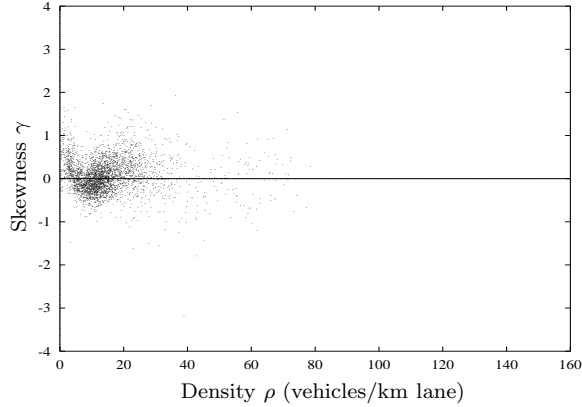


Fig. 5. The empirical skewness (\cdot) is approximately zero most of the time.

Moreover, it is interesting to know the variance-density relation (Fig. 7). Looking at the *temporal* evolution of the variance, one detects significant peaks when the average velocity breaks down or recovers (Fig. 8). Detailed mathematical considerations show (Helbing, 1997), that it can be reconstructed from the temporal course of the vehicle density $\rho(x, t)$ via the variance-density relation $\Theta_e(\rho)$, if one takes into account a positive correction term which is caused by averaging over finite time periods T . The theoretical relation reads

$$\Theta(x, t) \approx \Theta_e(\rho(x, t)) + \frac{T^2}{4} \left(\frac{\partial V}{\partial t} \right)^2. \quad (7)$$

Investigating the temporal fluctuations of the average velocity $V(x, t)$, one finds a flat power spec-

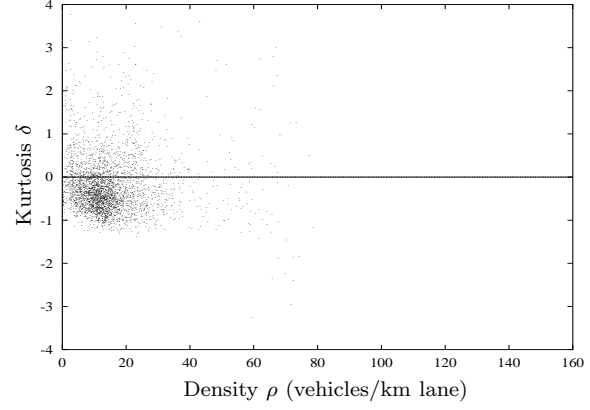


Fig. 6. The empirical kurtosis shows a small systematic deviation from zero due the finite truck fraction. Nevertheless, it is almost zero.

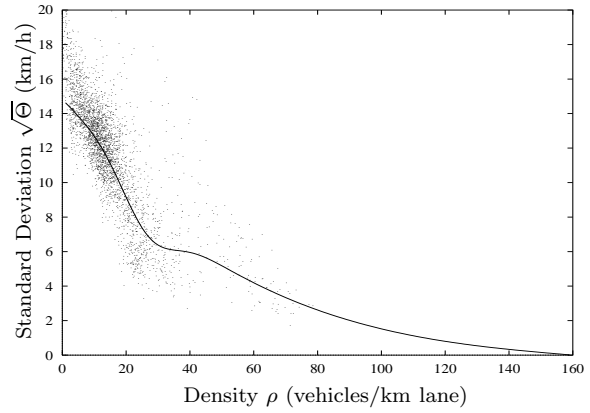


Fig. 7. Standard deviation $\sqrt{\Theta(x, t)}$ of vehicle velocities in dependence of density $\rho(x, t)$ (\cdot) and corresponding fit function $\sqrt{\Theta_e(\rho)}$ ($-$).

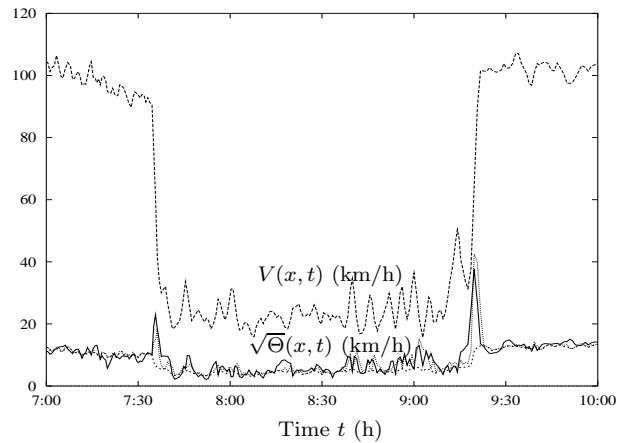


Fig. 8. The standard deviation $\sqrt{\Theta(x, t)}$ of vehicle velocities ($-$) has maxima, when the average velocity $V(x, t)$ ($--$) changes considerably. It cannot be described by the variance-density relation $\sqrt{\Theta_e(\rho(x, t))}$ alone (\cdots), but together with an additional positive term which arises from the evaluation procedure (\cdots).

trum $\hat{V}(\nu)$, i.e. almost the same intensity of the different fluctuation frequencies, corresponding to a so-called “white noise” (Fig. 9). However, at small frequencies ν (large oscillation periods $1/\nu$) the power law

$$\hat{V}(\nu) = C\nu^{-2} \quad (8)$$

appears. Similar results are obtained for the fluctuations of the density $\rho(x, t)$ or the variance $\Theta(x, t)$. The power law behavior is most distinct near to entrances, but only weakly visible at undisturbed sections of the freeway.

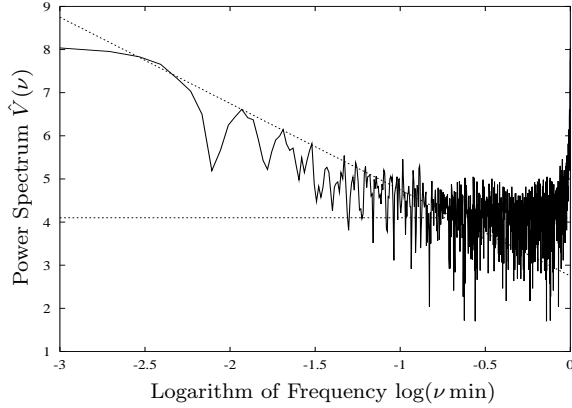


Fig. 9. Power spectrum of the average velocity's temporal course (—: $\log C - \delta \log \nu$, $\delta \in \{0, 2\}$).

It has also been found that the dynamics on neighboring lanes is strongly correlated (Fig. 10).

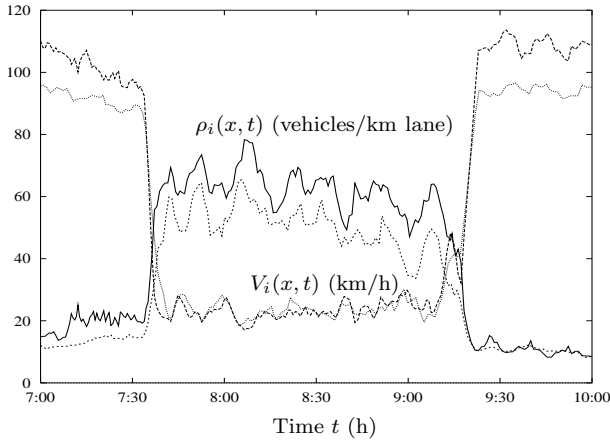


Fig. 10. Comparison of the temporal course of the vehicle density $\rho_i(x, t)$ on the left lane (—) with the right lane (---) and of the average velocity $V_i(x, t)$ on the left lane (---) with the right lane (···).

This justifies the common practice to model the dynamics of the total cross section of the road in an overall manner, treating it like a single lane with higher capacity and possibilities of overtaking (instead of explicitly describing the dynamics of *all* the lanes, including their interactions by overtaking and lane-changing maneuvers). Above

an average density of 35 vehicles per kilometer and lane the velocity on the left lane is the same as on the right lane, but the left lane is more crowded than the right one. The variance on neighboring lanes behaves almost identical (Helbing, 1997).

The maximum flow is 2200 vehicles per hour and lane, and it is reached at a density of 30 vehicles per kilometer and lane. Above this density, traffic flow breaks down and stop-and-go traffic develops. However, the hysteresis curve in Fig. 11 indicates that traffic flow is already unstable at densities of about 12 vehicles per kilometer and lane.

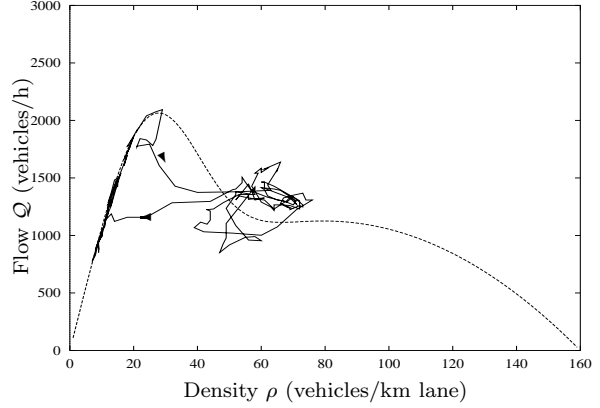


Fig. 11. Comparison of the fundamental diagram $Q_e(\rho)$ (—, cf. Fig. 2) with the temporal evolution of traffic flow $Q(x, t)$ (—).

Although the average velocity $V(x, t)$ recovers after a bottleneck (at $x = 0$ km), the amplitude of the emerging stop-and-go waves becomes larger and larger (Fig. 12). At the same time their wave length grows, indicating a merging of traffic jams.

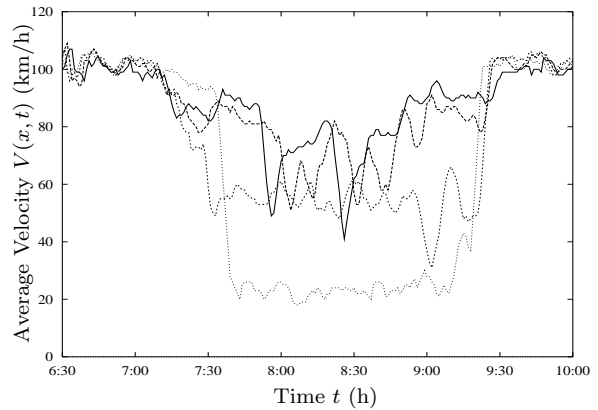


Fig. 12. Temporal evolution of the average velocity $V(x, t)$ at successive cross section of the freeway (···: $x = 0$ km; ---: $x = 0.95$ km; —·—: $x = 2.15$ km; —: $x = 4.15$ km).

3. CONSISTENT TRAFFIC MODELING

For a realistic description of traffic dynamics, it is sufficient to restrict the model to the continuity equation

$$\frac{\partial \rho}{\partial t} + \frac{\partial(\rho V)}{\partial x} = 0 \quad (9)$$

for the vehicle density $\rho(x, t)$ and a suitable dynamic equation for the average velocity $V(x, t)$. The velocity equation is necessary for the delineation of emergent traffic jams and stop-and-go traffic. The dynamics of the variance can be reconstructed from the temporal evolution of the density and average velocity according to Eq. (7). Due to the strong correlation between neighboring lanes, an overall description of the total road cross section is possible as long as the number of lanes does not change. Nevertheless, models for the interaction between neighboring lanes have also been built and simulated (Helbing, 1997).

It can be shown that the velocity equations of most previous macroscopic traffic models (in their continuous version) can be written in the form

$$\frac{\partial V}{\partial t} + V \frac{\partial V}{\partial x} = -\frac{1}{\rho} \frac{\partial \mathcal{P}}{\partial x} + \frac{1}{\tau} [V_e(\rho) - V]. \quad (10)$$

The main difference is the specification of the traffic pressure \mathcal{P} , the relaxation time τ and the velocity-density relation $V_e(\rho)$. For example, the Lighthill-Whitham model results in the limit $\tau \rightarrow 0$. Payne's and Papageorgiou's model is obtained for $\mathcal{P} = -V_e/2\tau$. For $d\mathcal{P}/d\rho = -\rho/[2\tau(\rho + \kappa)]dV_e/d\rho$ one ends up at Cremer's model. In the model of Phillips there is $\mathcal{P} = \rho\Theta$, where Θ denotes the velocity variance. The model of Kühne, Kerner and Konhäuser (Fig. 13) results for $\mathcal{P} = \rho\Theta_0 - \eta\partial V/\partial x$, where Θ_0 is a positive constant and η a viscosity coefficient.

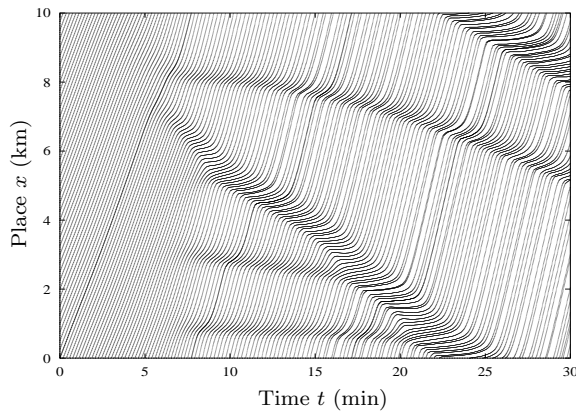


Fig. 13. The representative streamlines related to the simulation of the Kerner-Konhäuser model indicate the average velocity by their slope and the vehicle density by the line density. Starting with an almost homogeneous traffic situation with a density of 40 vehicles per kilometer and lane, density clusters (which correspond to traffic jams) develop in the course of time. These merge into greater clusters in agreement with Fig. 12.

All these models have proved their value in many applications, and it is hard to decide which is the best one. Nevertheless, recently these models have seriously been criticized by Daganzo and others. Therefore, a new macroscopic model has been derived from Boltzmann-like kinetic traffic equations, basing on a microscopic model of the dynamics of driver-vehicle units. The kinetic traffic model is related to Pavari-Fontana's one, but it additionally takes into account vehicular space requirements (by applying the Enskog-formalism for dense gases) and velocity fluctuations due to imperfect driving (Helbing, 1997).

The calculation of the corresponding macroscopic traffic equations is very laborious. For the equilibrium velocity one finds the relation

$$V^e(\rho, V, \Theta) = V_0 - \frac{\tau(\rho)[1 - p(\rho)]\rho\Theta}{1 - \rho/\rho_{max} - \rho T_r V}, \quad (11)$$

where V_0 is the average desired velocity, $p(\rho)$ the probability of immediate overtaking, $\rho_{max} \approx 160$ vehicles per kilometer and lane the maximum vehicle density, and $T_r \approx 0.8$ s the reaction time. The equilibrium variance $\Theta^e(\rho, V, \Theta) = A(\rho)(V^2 + \Theta)$, where $A(\rho)$ denotes the strength of velocity fluctuations, vanishes with the average velocity V , as required. Utilizing these relations, it is possible to reconstruct the velocity-density relation $V_e(\rho) = V^e(\rho, V^e, \Theta^e)$ (Fig. 1) and the variance-density relation $\Theta_e(\rho) = \Theta^e(\rho, V^e, \Theta^e)$ (Fig. 7) at high densities ρ (Helbing, 1997). Applying the equilibrium approximation

$$\begin{aligned} \Theta(x, t) &\approx \Theta^e(\rho(x, t), V(x, t), \Theta^e(x, t)) \\ &= \frac{A(\rho(x, t))[V(x, t)]^2}{1 - A(\rho(x, t))}, \end{aligned} \quad (12)$$

one finally arrives at the corrected velocity equation

$$\begin{aligned} \frac{\partial V}{\partial t} + V \frac{\partial V}{\partial x} &= -\frac{1}{\rho} \frac{\partial \mathcal{P}}{\partial \rho} \frac{\partial \rho}{\partial x} + a \frac{\partial V}{\partial x} - b \frac{\partial^2 \rho}{\partial x^2} \\ &\quad + \frac{\eta}{\rho} \frac{\partial^2 V}{\partial x^2} + \frac{1}{\tau} [V^e(\rho, V) - V]. \end{aligned} \quad (13)$$

Comparing this with (10), one obviously obtains the additional terms $a\partial V/\partial x$ and $-b\partial^2 \rho/\partial x^2$. Moreover, \mathcal{P} , η , V^e , a , and b are not only functions of the density ρ anymore, but they also depend on the average velocity V . The corresponding functional relationships can be analytically derived, and the model parameters have been determined from empirical data.

It can be shown that the model automatically meets all consistency criteria: 1. The equilibrium velocity $V^e(\rho, V)$ decreases monotonically with growing density ρ and vanishes at the maximum vehicle density ρ_{max} . 2. Since $\partial \mathcal{P}/\partial \rho$ and b vanish

for $V = 0$, the average velocity V cannot become negative. 3. Since $\partial \mathcal{P} / \partial \rho$ is non-negative (Fig. 14), the traffic pressure monotonically increases with the density ρ . As a consequence, vehicles will not accelerate in direction of growing density ($\partial \rho / \partial x > 0$). 4. The traffic pressure

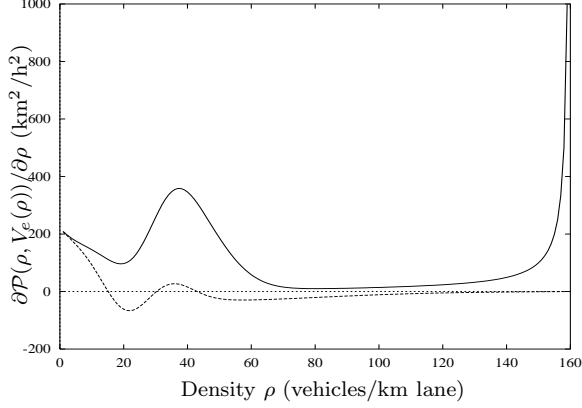


Fig. 14. Representation of the density-gradients of the *idealized* traffic pressure $\mathcal{P} = \rho \Theta_e(\rho)$ of point-like vehicles (—) and the *corrected* pressure relation (—) which takes into account their finite space requirements.

diverges at $\rho = \rho_{max}$. For this reason, the maximum density ρ_{max} cannot be exceeded. 5. The viscosity η (Fig. 15) is theoretically explained. Its divergence at $\rho = \rho_{max}$ guarantees that velocity changes are smoothed out, so that the development of shock-like structures is avoided and numerical integration methods are stable. 6. The

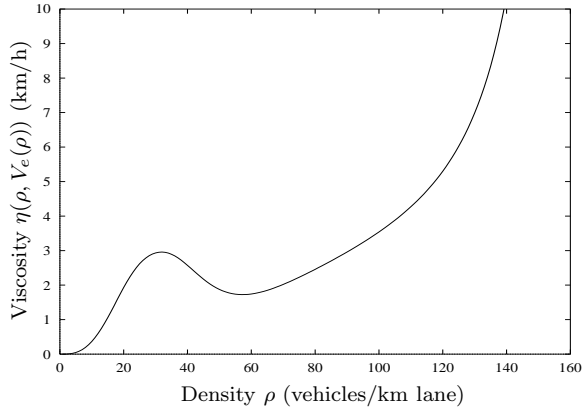


Fig. 15. Representation of the theoretically obtained viscosity function.

traffic flow is found to be stable at small and extreme densities, otherwise unstable (Fig. 16a). The result is in good agreement with Fig. 11. Therefore, the development of stop-and-go waves from almost homogeneous traffic conditions is correctly described. The propagation velocity of the evolving density waves (Fig. 16b) has the right order of magnitude and direction, i.e. stop-and-go-waves move in backward direction with respect to the average velocity V .

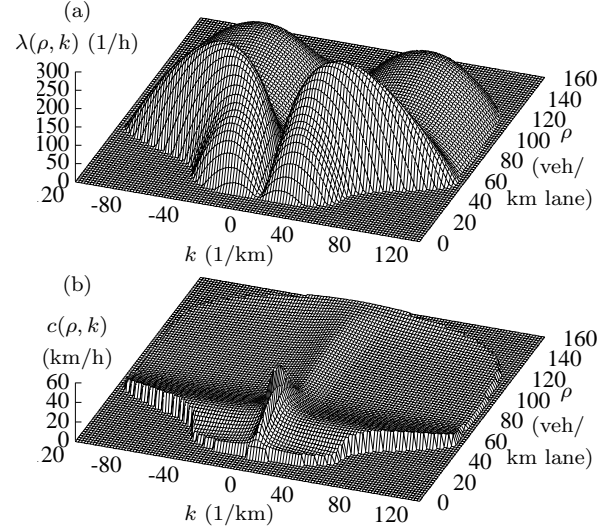


Fig. 16. The illustrations show (a) the growth rate λ and (b) the relative backward propagation velocity c of small periodic disturbances with wave number k (corresponding to a wave length of $\ell = 2\pi/k$), where the homogeneous traffic flow at density ρ is unstable.

4. SUMMARY AND CONCLUSIONS

Empirical traffic data have been compared to results of recent macroscopic traffic models. The following has been found: 1. Vehicle velocities are approximately normal distributed. This can be explained by an improved kinetic model. 2. The dynamics on neighboring lanes is strongly correlated so that the total freeway cross section can be described in an effective way. 3. The distance between forming stop-and-go waves increases in the course of time, which corresponds to the merging of density clusters in traffic simulations. 4. The dynamical variance has peaks when the velocity changes considerably. It can be approximated by the variance-density relation and an additional term which arises from averaging the vehicle data over finite time intervals. 5. The fluctuations of traffic density and average velocity essentially correspond to a white noise. 6. Traffic flow is unstable above a density of about 12 vehicles per kilometer and lane. This can be understood by means of a linear stability analysis of a new macroscopic traffic flow model which has been derived from the dynamics of driver-vehicle units via an improved kinetic model. 7. The model allows to reconstruct the velocity-density and variance-density relations at high densities and takes into account velocity fluctuations as well as the finite space requirements of vehicles.

5. REFERENCES

Helbing, D. (1997). *Verkehrsdynamik: Neue physikalische Modellierungskonzepte*. Springer. Berlin.